Received <day> <Month>, <year>; | Revised <day> <Month>, <year>; | Accepted <day> <Month>, <year>

DOI: xxx/xxxx

ARTICLE TYPE

Multi-parametric analysis of the chaotic dynamic behavior of the Alpazur oscillator

DINGAMADJI Aristide[1] | DJONDINE Philippe*[1,2] | GUIDKAYA GOLAM[1]

[1]Department of physics, Faculty of Science, The University of Ngaoundéré, P.O. Box 454, Cameroon

[2]Department of physics, Higher Teacher Training College, The University of Bertoua, P.O. Box 652, Cameroon

Correspondence
*Philippe Djondiné, Email: pdjondine@yahoo.fr

Abstract

In this parper we consider an Alpazur oscillator which consists of a Rayleigh-type oscillator and a DC power supply controlled by a switch that modifies the operating mode. The oscillator denotes some special phenomena in some parameter settings and are called chaos or bifurcation. In addition, we observe the behavior of this oscillator over a wide rage of parameter variation. Chaos theory tools such as, bifurcation, phase portrait, poincaré section and Matching Energy (ME) was examined in the analysis of dynamic of the system. Simulations were carried out using the 4^{th}-order Runge-Kutta algoritm in Matlab. The results shows that Alpazur oscillator is sensitive to parameter variation and exhibts a wide range dynamics from fundamental periodicty to chaos.

KEYWORDS:
Alpazur oscillator, switching operation, multi-parametric bifurcation, Matching Energy

1 | INTRODUCTION

Research into nonlinear dynamical systems made remarkable progress in the 1970s with pioneering work such as Edward Lorenz's discovery of the butterfly effect. This discovery highlighted the sensitivity of nonlinear dynamical systems to initial conditions, leading to the recognition of chaotic behavior in physical dynamical systems. Since then, various research works have confirmed the presence of chaotic behavior in a variety of disciplines, such as physics, engineering, chemistry, biology and so on [1], [2], [3]. However, it is electronic circuits that have played an important role in the attempt to understand the chaotic phenomenon and to elaborate the properties of chaos. The electrical circuits including switching actions are discussed as a recent interesting subject of search in much of previous works [4], [5], [6], [7]. Circuits with one or more switches, also called on-off circuits, are generally described by dynamical differential equations switched in certain manner typically synchronous or asynchronous modes. In synchronous modes, the switching is done by a periodic external independent state excitation [8], [9]. Whereas in asynchronous mode, toggling is controlled by a depending state excitation [10], [11]. Thus a switching circuit can be described as piecewise switched circuit which assumes different topologies at different times [12]. However, they also offer the possibility of integration in various fields of application: communications security, cryptography, random noise generation, etc. The oscillator of one of the most famous researchers in chaos theory, Léon Chua, became a paradigm for chaos [13]. During this time, a number of methods and tools have been developed that have contributed to the study and understanding of the behavior of nonlinear dynamical systems. These include the Lyapunov exponent, which measures sensitivity to initial conditions in nonlinear dynamic systems. The phase portrait and the Poincaré section, which can be used to graphically represent and observe limit cycles and sub-harmonic behavior and the bifurcation diagram, which can be used to study behavior under variation of a parameter. In this paper, the dynamic behavior of the Alpazur oscillator is studied under the variation of several

parameters. Multi-parametric analysis explores the complex interactions between the system's state variables and the parameters governing its dynamics. It identifies regions of stability, bifurcations, periodic behavior and sensitivities to parameter variation. To explore the dynamics of the Alpazur oscillator, we use tools such as the bifurcation diagram and the quantitative Matching Energy approach, which is a technique used to numerically evaluate the occurrence or non-occurrence of chaos in nonlinear dynamical systems. For numerical resolution, the Runge-Kutta fixed-step 4th-order algorithm is used. The manuscript is structured as follows: section is mainly indended to describe the Alpazur oscillator. Section 3 is devoted to present the numerical resolution approach using Runge-Kutta of four order. Section 4 is devoted to present two different methods analysing chaotic behaviors. In section 5 we have simulation results.

2 | MODEL PRESENTATION

We consider a model *RLC* oscillator circuit containing a nonlinear characteristic (nonlinear resistance), and a DC power supply controlled by a switch as shown in figure 1 . This oscillator is a power electronic circuit introduced by Kawakami and Lozi [14]. It consists of a Rayleigh oscillator block and a DC power supply controlled by a switch (itself controlled by a feedback loop). Although a non-linear resistor is rare in real applications, this simple circuit is non-linear in parts, and can exhibit chaotic behavior for some of its parameters.

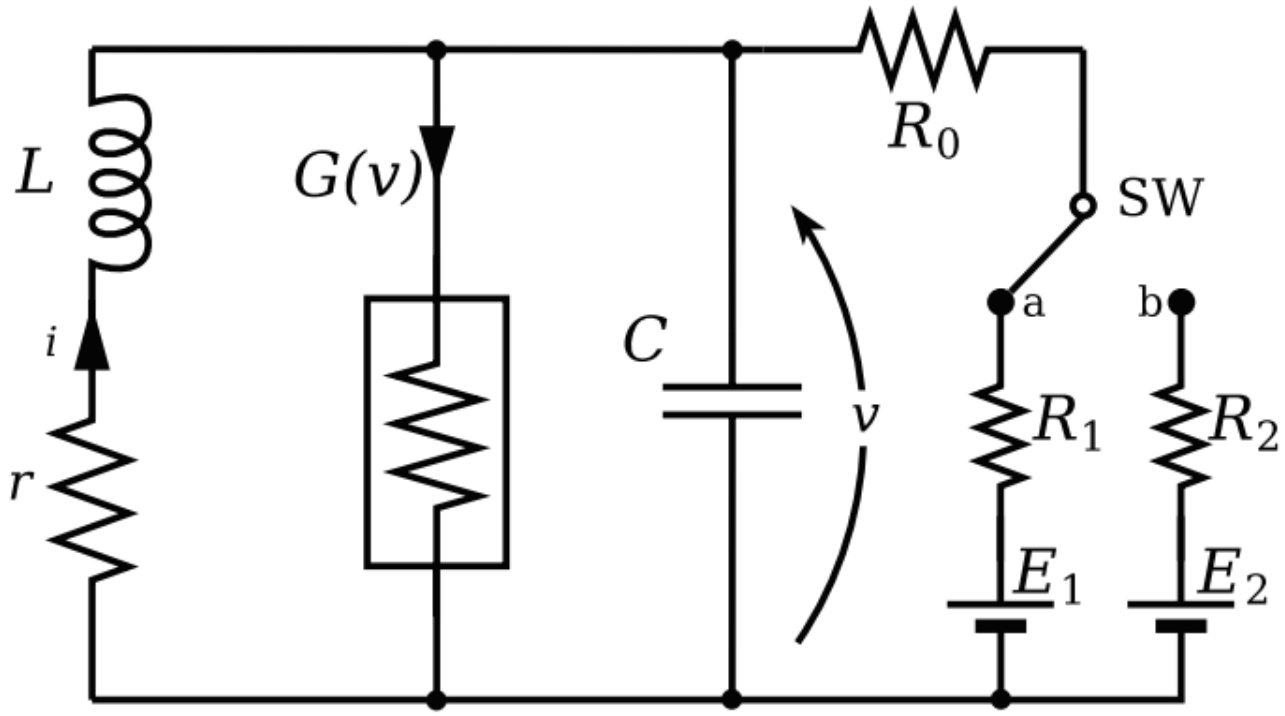

FIGURE 1 Alpazur 2-state oscillator circuit

The circuit's operating mode is modified by the ***SW*** switch, which can assume the ***a*** and ***b*** positions shown in figure **??**. The switching period is noted ***T***. The ratio of switching times for which the switch remains in position ***a*** and ***b*** is denoted $\boldsymbol{\theta}$. In what follows, we'll look at the various points that enable us to mathematically define the set of equations governing the operation of

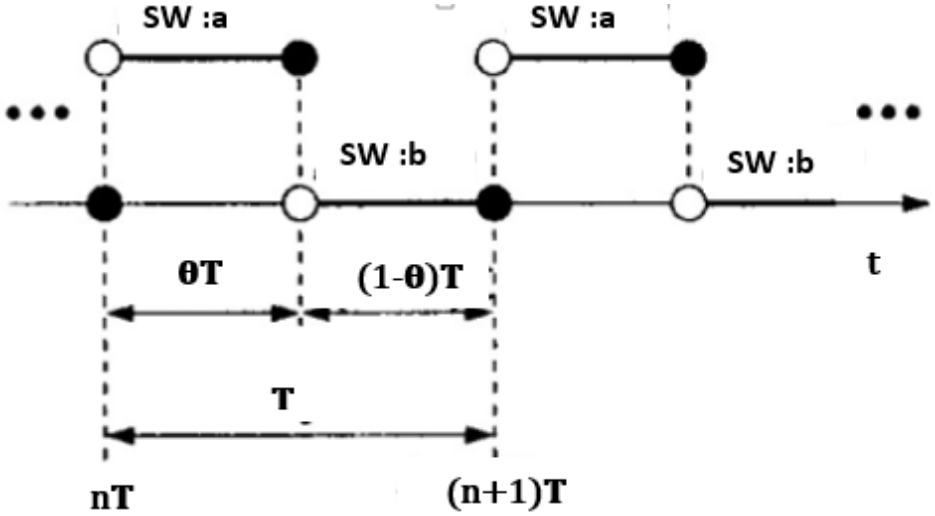

FIGURE 2 Chronogram of the switch excitation

the figure 1 . Applying Kirchhoff's laws: the whole system can be described by the following systems of equations:

$$\begin{cases} L\frac{di}{dt} & = -ri - v \\ C\frac{dv}{dt} & = i - G(v) + \frac{E_j - v}{R_j + R_0} \end{cases} \qquad \text{j=1,2} \tag{1}$$

The transition from one switch state to the other is shown in figure **??**. The changeover condition is determined by θ

When the switch is connected to the ***a*** side, the circuit equation is given by :

$$\begin{cases} L\frac{di}{dt} & = -ri - v \\ C\frac{dv}{dt} & = i - G(v) + \frac{E_1 - v}{R_1 + R_0} \end{cases} \quad 0 < t \leq \theta T \tag{2}$$

When the switch is connected to ***b*** side, the circuit equation is given by:

$$\begin{cases} L\frac{di}{dt} & = -ri - v \\ C\frac{dv}{dt} & = i - G(v) + \frac{E_2 - v}{R_2 + R_0} \end{cases} \quad \theta T \leq t < T \tag{3}$$

$$\begin{aligned} &\hat{x} = \sqrt{L}i; \qquad \hat{y} = \sqrt{C}v; \qquad t' = \frac{1}{\sqrt{LC}}t; \\ &r_1 = \frac{1}{R_1 + R_0}; \qquad r_2 = \frac{1}{R_2 + R_0}; \qquad k = r\sqrt{\frac{C}{L}} \\ &A_1 = 1 - (a_1 - r_1)\sqrt{\frac{L}{C}}; \qquad A_2 = 1 - (a_1 - r_2)\sqrt{\frac{L}{C}}; \qquad C_3 = \frac{3a_3}{C}\sqrt{\frac{L}{C}} \\ &\hat{B}_1 = r_1\sqrt{L}E_1; \qquad \hat{B}_2 = r_2\sqrt{L}E_2; \end{aligned} \tag{4}$$

By replacing the new variables in the equations and relabeling t' as t, the equations (2) and (3) are transformed and the following differential equations are obtained:

$$sw : a \begin{cases} \frac{dx}{dt'} & = -kx - y \\ \frac{dy}{dt'} & = x + (1 - A_1)y - \frac{1}{3}y^3 + B_1 \end{cases} \quad 0 < t \leq \theta T \tag{5}$$

$$sw : b \begin{cases} \frac{dx}{dt'} & = -kx - y \\ \frac{dy}{dt'} & = x + (1 - A_2)y - \frac{1}{3}y^3 + B_2 \end{cases} \quad \theta T \leq t < T \tag{6}$$

3 | RESOLUTION APPROACH

An immeasurable amount of research and publication has been devoted to the numerical solutions of both ordinary and partial differential equations (ODEs and PDEs). An ordinary differential equation (ODE) is an equality involving a function and its derivatives. Although there are many general techniques for analytically solving classes of ODEs, the only practical solution is numerical solution. The use of numerical methods is the most common [15] technique for solving complex equations in physics, engineering, economics and electronics. The most popular of these are the Runge-Kutta (RKM) methods. The Runge-Kutta method can be used to solve differential equations of the following form:

$$\begin{cases} \frac{dy}{dx} & = f(x, y) \\ y(x_0) & = y_0 \end{cases} \tag{7}$$

The solution to this equation is given by:

$$y(x + h) = y(x) + \frac{1}{6}(k_1 + 2k_2 + 2k_3 + k_4) \tag{8}$$

où

$$\begin{aligned} k_1 &= hf(x, y(x)) \\ k_2 &= hf(x + \frac{1}{2h}, y(x) + \frac{k_1}{2}) \\ k_3 &= hf(x + \frac{1}{2}h, y(x) + \frac{k_3}{2}) \\ k_4 &= hf(x + h, y(x) + k_3) \end{aligned} \tag{9}$$

Thus, the next value $y(x + h)$ is determined by the current value $y(x)$ plus an estimate of the slope (k_1, k_2, k_3, k_4). The slope is a weighted mean slope. The total accumulated error is of the order of h^4.

4 | ALNALYSIS TOOLS PRESENTATION

4.1 | Qualitative analysis

Qualitative analysis uses subjectives judgment based on soft or non quantifiable data. Qualitative analysis deals with intangible and inexact information that can be difficult to collect and measure. Qualitative analysis of dynamic systems aims to understand the overall behavior in order to observe the system's behavior we need analysis tools such as the bifurcation diagram, the Poincaré section, the phase portrait and the time response.

4.2 | Analyse quantitative of Matching Energy (ME)

The ME [16] approach for detecting the behavior of a nonlinear dynamic system using a set of system simulation data is briefly described in this subsection. Consider a data series $x_t, t = 0, 1, 2, \ldots, T-1$, of size T. Let P_t be a vector obtained by rearranging in ascending order the values of x_t, and Q_t a vector obtained by rearranging in descending order x_t. From the series x_t, P_t, Q_t, we derive the data vectors

$x_k = \left(x_{k\tau_0}, x_{k\tau_0+1}, \ldots, x_{k\tau_0+n-1}\right), p_k = \left(x_{k\tau_0}, p_{k\tau_0+1}, \ldots, p_{k\tau_0+n-1}\right)$

et $q_k = \left(x_{k\tau_0}, q_{k\tau_0+1}, \ldots, q_{k\tau_0+n-1}\right)$, size n, où n is an integer less than T, et $1 \leq \tau_0 \leq n$. The ME approach involves projecting x_k, p_k, and q_k onto two vector subspaces $V^{(1)}$ and $V^{(2)}$. Let y_k and z_k be two sets of data obtained respectively by rearranging in ascending and descending order the vector $x_k; n_1$ is the number of coordinates between y_k and p_k, possessing the same values while n_1^{prime} is the number of coordinates between z_k and q_k possessing the same values. Considering $x_k^{(1)}$ and $x_k^{(2)}$ the respective projections of x_k onto the subspaces $V^{(1)}$ and $V^{(2)}$, the corresponding energies E_k^- and E_k^+ in these two subspaces are given by the equations 10 and 11 respectively:

$$E_k^- = \sqrt{\frac{1}{n_1}\sum_{i=1}^{n_1}\left[x_k^{(1)}(i) - \overline{x_k^{(1)}}\right]^2} \tag{10}$$

$$E_k^+ = \sqrt{\frac{1}{n - n_1}\sum_{i=1}^{n-n_1}\left[x_k^{(2)}(i) - \overline{x_k^{(2)}}\right]^2} \tag{11}$$

where $\overline{x_k^{(1)}}$ and $\overline{x_k^{(2)}}$ are respectively the mean value of x_k in the vector subspaces $V^{(1)}$ and $V^{(2)}$. The mean distance (or mutual energy) for coordinates with non-identical values between y_k and p_k, z_k and q_k is given by the following relation 12:

$$d_{k+} = \frac{1}{2}\left[d_{k+}^{(p)} + d_{k+}^{(q)}\right] \tag{12}$$

Avec $d_{k+}^{(p)}$ et $d_{k+}^{(q)}$ donnés par :

$$d_{k+}^{(p)} = \sqrt{\frac{1}{n-n_1}\sum_{i=1}^{n-n_1}\left[y_k^{(2)}(i) - \overline{p_k^{(2)}}\right]^2} \tag{13}$$

$$d_{k+}^{(q)} = \sqrt{\frac{1}{n-n_1'}\sum_{i=1}^{n-n_1'}\left[z_k^{(2)}(i) - \overline{q_k^{(2)}}\right]^2} \tag{14}$$

Since the average distance between coordinates with identical values between y_k and p_k, z_k and q_k is zero, then the energy E_k^- is not involved in the calculation of the total energy. The partial energy associated with the k^{gravee} element of x_k, p_k and q_k derived respectively from x_t, p_t and q_t, is given by :

$$E_k(n) = \begin{cases} 0, & \text{si } \left(n_1 + n_1'\right) \neq 0 \\ E_k^+, & \text{si } \left(n_1 + n_1'\right) = 0 \end{cases} \tag{15}$$

Finally, the translation of the complexity or otherwise of the data series in question is given by the equation 16 :

$$E(n) = \frac{1}{N}\sum_{k=1}^{N} E_k(n) \tag{16}$$

with :

$$N = 1 + \text{ floor}\left(\frac{T-n}{\tau_0}\right) \tag{17}$$

Thus, for a zero value of $E(n)$, the system's behavior is perfectly predictable, so the system is periodic and its dynamics are regular. On the other hand, for a non-zero value of $E(n)$, the system's behavior is not predictable. In other words, the system's dynamics include an infinite number of operating periods, a phenomenon characteristic of chaotic behavior.

5 | SIMULATION RESULTS

Solving differential equations is the most important ordinary technique. Numerical integration provides the necessary information on the dynamic behavior of the system. We use the RK numerical integration method, which is highly accurate and less time-consuming to calculate [17]. To simulate the behavior of the Alpazur oscillator, we have used the Matlab numerical computation software. The system of differential equations governing the dynamic behavior of the Alpazur oscillator is numerically solved using the Runge-Kutta fourth-order fixed-step method. First we present a bifurcation diagram, which allows us to observe the critical values of the chosen parameters that influence the system's behavior. Then we give phase portraits, which allow us to accurately observe the behavior of a dynamic system by projecting it into the phase parameter space. The ME technique is applied to the Alpazur oscillator to observe its quantitative behavior, to see the intervals of values of each parameter for which the system is chaotic or periodic.the values of the actual circuit parameters of the figure 1 are taken from [17] .

5.1 | Analysis of oscillator behavior under variation of θ parameter

In this section we present the simulation results under variation of the parameter θ,this parameter which defines the switching motion is described in figure 2 . In order to observe the behavior of the Alpazur oscillator under variation of this parameter, we present the bifurcation diagram accompanied by the Matching Energy, followed by the time responses, the phase portrait and the Poincaré cross-section for a selected range of θ values.

5.1.1 | Bifurcation diagram

The bifurcation diagram presented here shows the evolution of the state variable x under variation of the parameter θ. Simulations are performed over a range of θ values from 0.82 to 0.90 in 10^{-4} steps. For each value of θ, 1700 periods of circuit operation

were recorded with a resolution of 10000 points per period. In order to eliminate as many transient values as possible for each value of θ, only the last 750 periods were retained for the bifurcation diagram. The ME technique is applied to the Alpazur oscillator in order to present the behavior of its global dynamics. The results obtained are presented in the following section (figure 3). Observation of figure 4 shows that for θ values below 0.88 the oscillator's dynamics exhibit periodic behavior

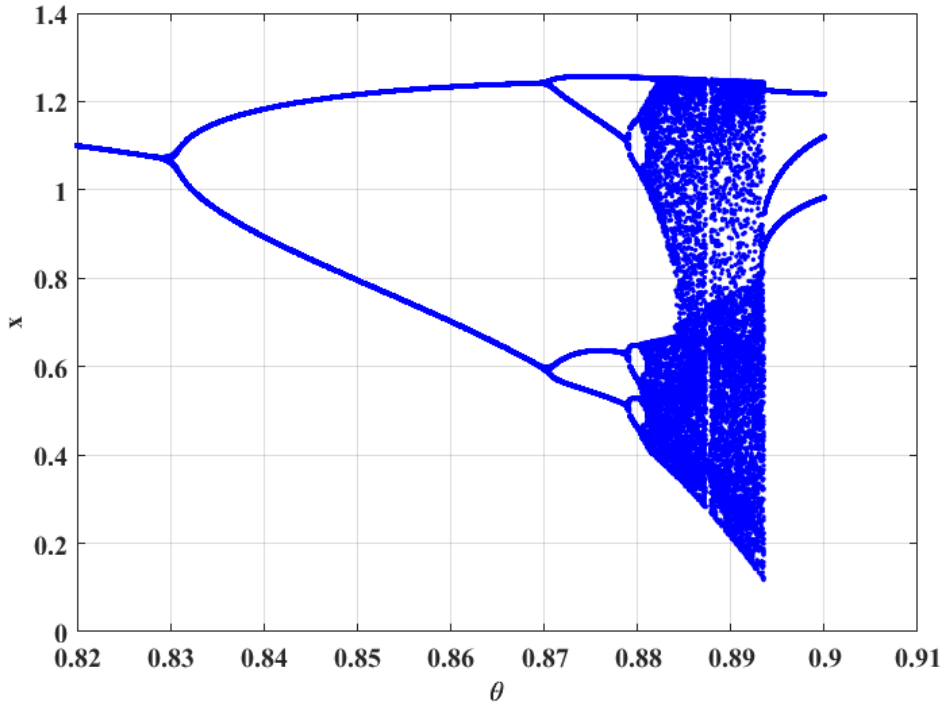

FIGURE 3 Bifurcation of x

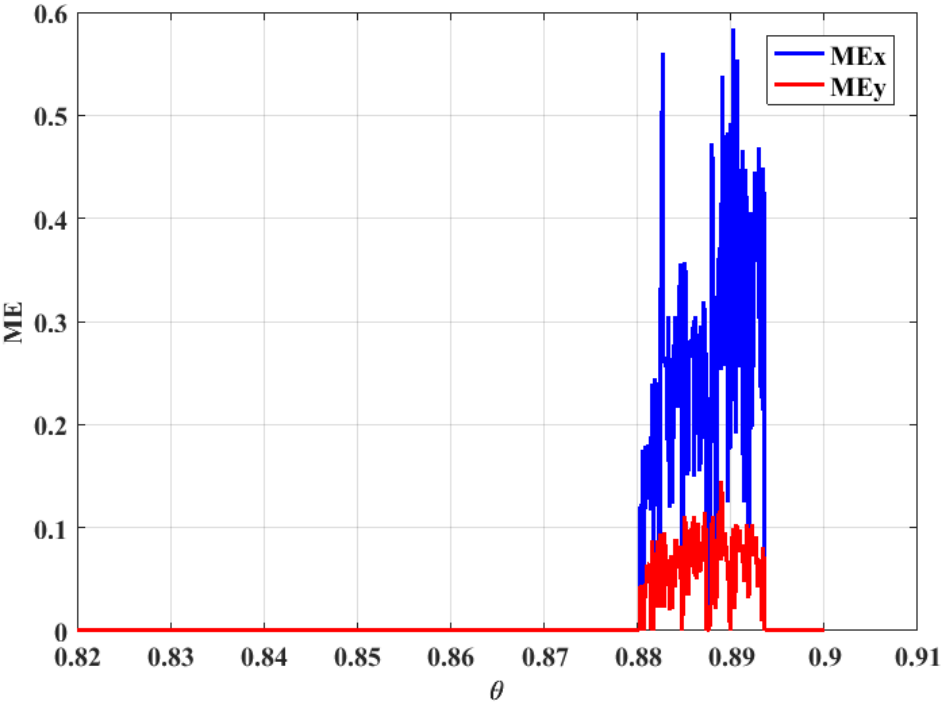

FIGURE 4 Matching Energy at θ

(since the calculated ME value is zero).for a non-zero ME value this state is characterized by chaotic dynamics. The Matching Energy (ME) approach clearly confirms the behavior observed on the bifurcation diagrams: for a zero ME value the oscillator dynamics is periodic, and for a non-zero ME value the behavior is chaotic.

5.1.2 | Temporal responses

In order to present the dynamic behavior of the Alpazur oscillator for a few values of θ taken from the previous bifurcation diagram, for each value of θ we present the time series, phase portrait and Poincaré section.

a) Behavior at $\theta = 0.825$

At this value of θ ,the oscillation dynamics presents a limit cycle ,observed on time evolution by the presence of regular periods at figure 5 . This behavior is confirmed by the phase portrait, which shows a limit cycle characteristic of fundamental periodic behavior figure 6 , confirmed by the Poincaré section with a single point figure 7 .

b) Behavior at $\theta = 0.875$

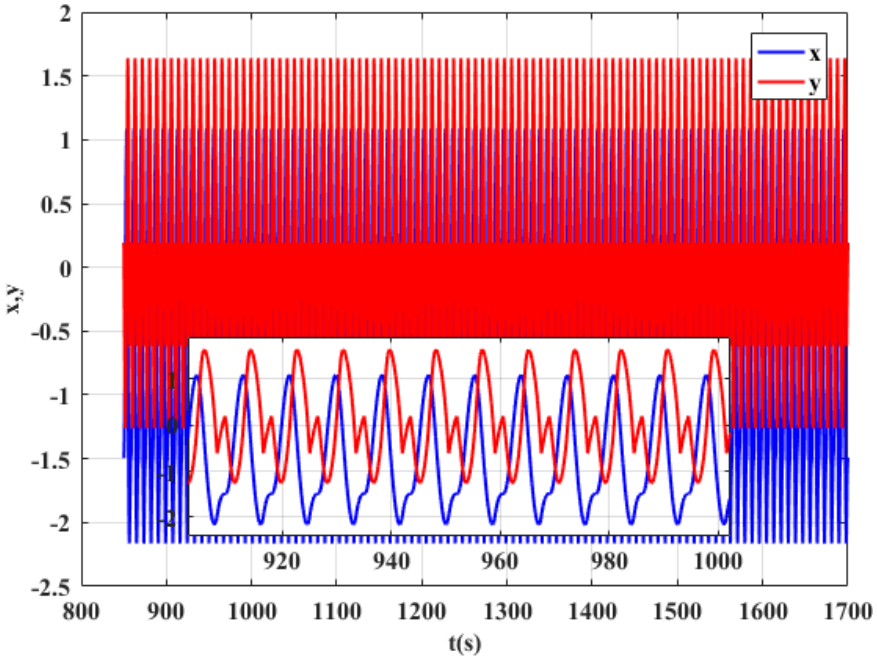

FIGURE 5 Temporal response for $\theta = 0.825$

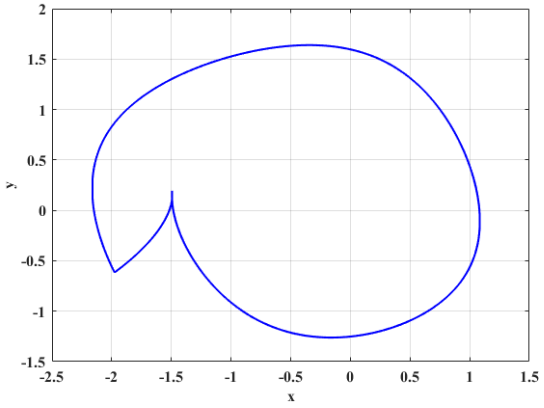

FIGURE 6 Phase portrait for $\theta = 0.825$

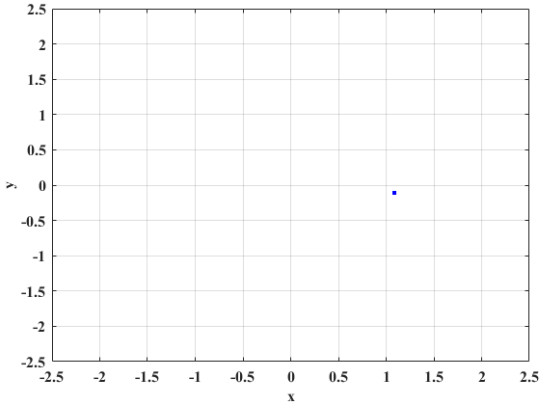

FIGURE 7 Poincaré section

The oscillator's behavior at this value of $\theta = 0.875$ shows a sub-harmonic behavior of rank 4, which shows a time evolution of four regular periods (figure 8). This behavior is observed by the presence of 4 cycles (figure 9) which is confirmed by the presence of the 4 points on the Poincaré section (figure 10).

c) Behavior at $\theta = 0.89$

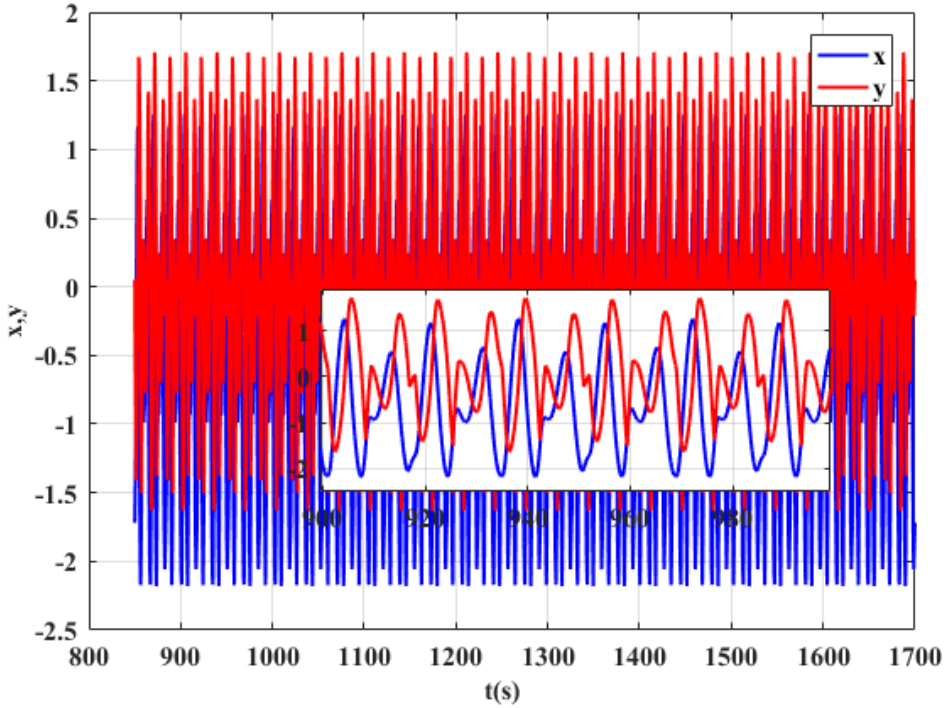

FIGURE 8 Temporal response for $\theta = 0.875$

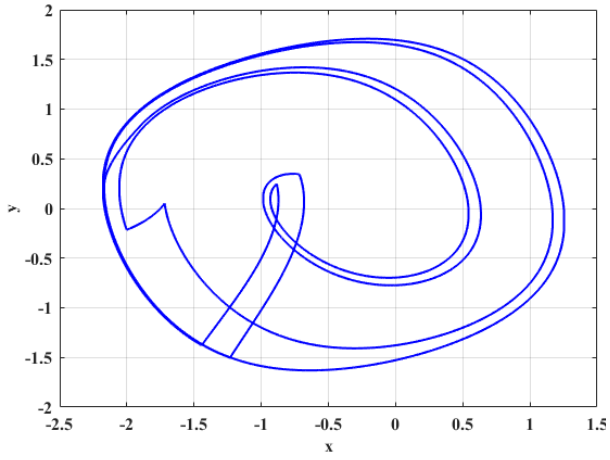

FIGURE 9 Phase portrait for $\theta = 0.875$

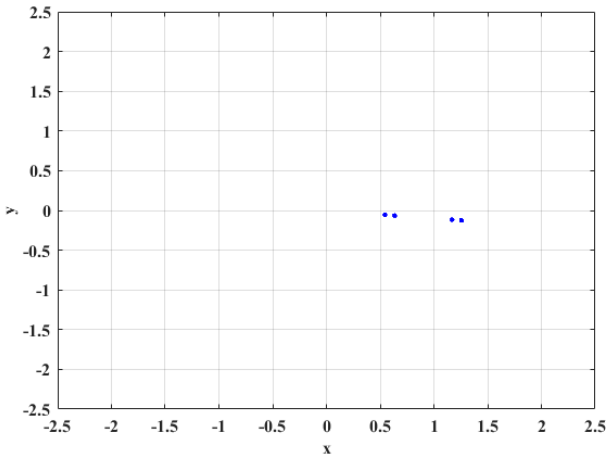

FIGURE 10 Poincare section

The dynamics of the oscillator for the value of θ taken in the chaotic zone from the bifurcation diagram and Matching Energy is presented in this section. The phase portrait (figure 12) shows a strange attractor that is characteristic of chaotic behavior, and the presence of several points on the Poincaré section (figure 13) indicates the existence of a period multiplicity. The oscillator exhibits chaotic behavior for this value of θ.

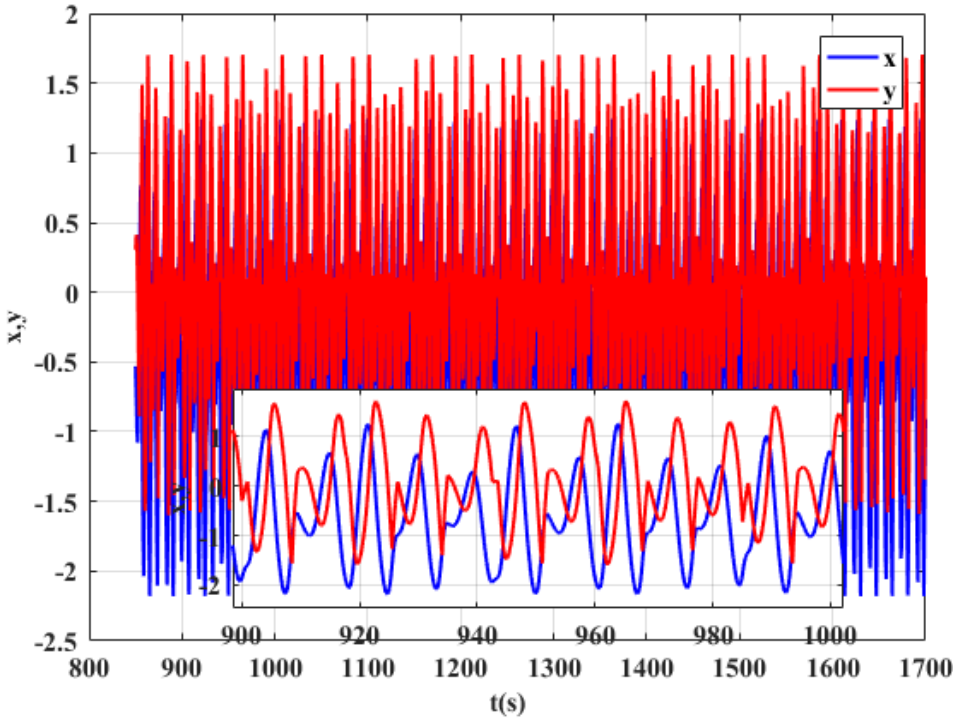

FIGURE 11 Temporal response for $\theta = 0.89$

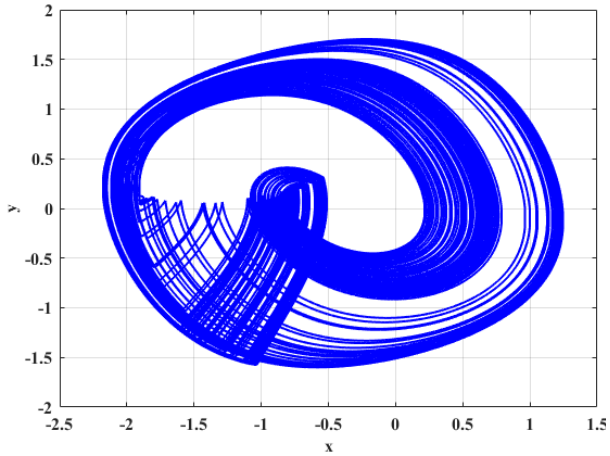

FIGURE 12 Phase portrait for $\theta = 0.89$

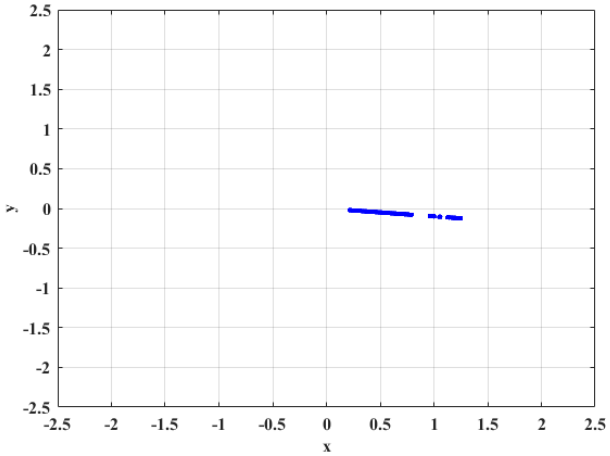

FIGURE 13 Poincaré section

5.2 | Analysis of oscillator behavior under parameter variation T

5.2.1 | Bifurcation diagram

The bifurcation diagram presented here shows the evolution of the state variable x under variation of the parameter T. This parameter defines the operating period of the switch, i.e. the switching time at points **a** and **b**. Simulations are performed over a range of T values from 0 to 8.5 in 10^{-4} steps. For each value of T 1700 periods of circuit operation were recorded with a resolution of 10000 points per period. In order to eliminate as many transient values as possible for each T value, only the last 750 periods were retained for the bifurcation diagram. The EM technique is applied to the Alpazur oscillator to present the quantitative behavior using the bifurcation diagram data. Looking at the bifurcation diagram in figure 14 for a certain value of T, the oscillator dynamics show chaotic behavior. For values of T greater than 4.7, the behavior is periodic, as confirmed by the Matching Energy approach. For a value of ME of zero, the behavior is periodic, and for a non-zero value, the behavior is chaotic.

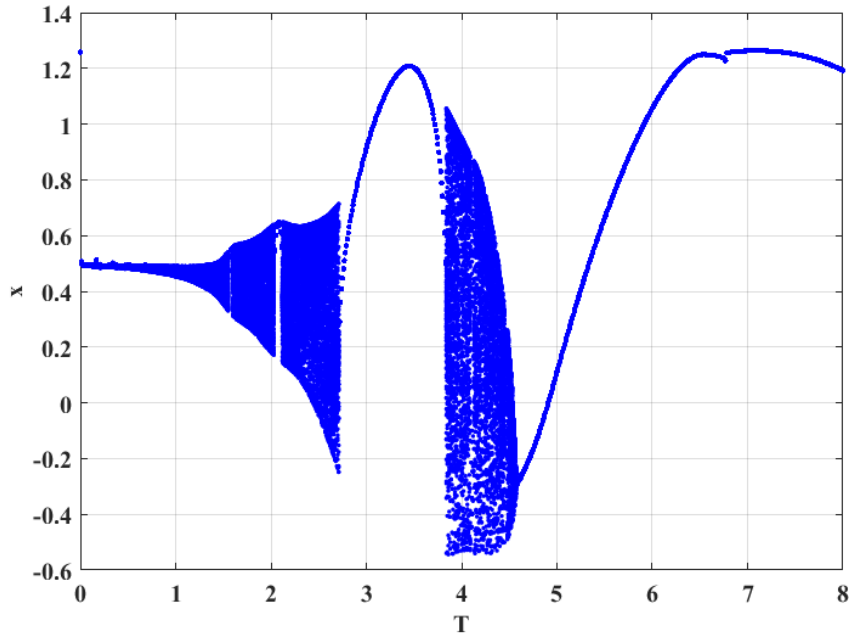

FIGURE 14 Bifurcation of x

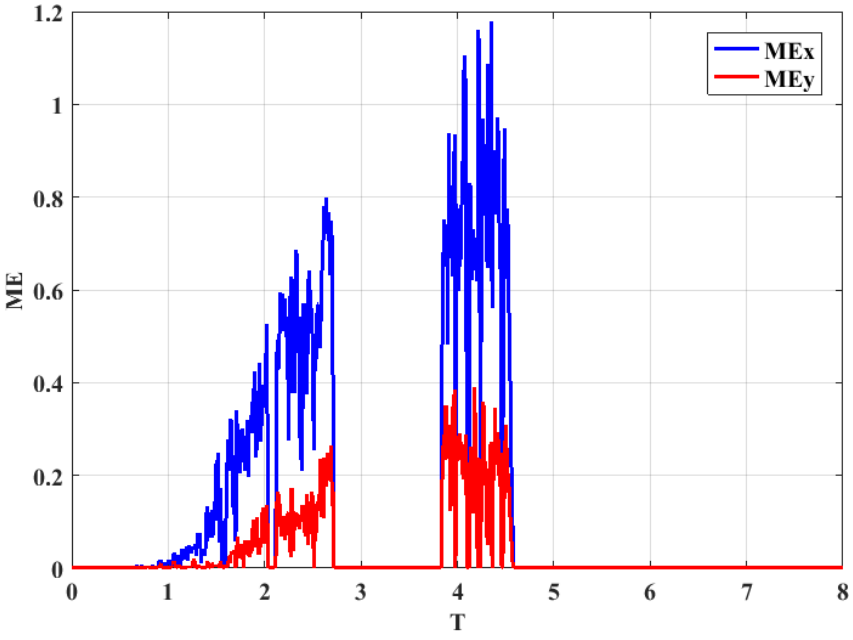

FIGURE 15 Matching Energy at θ

5.2.2 | Temporal responses

a) Behavior at $T = 4.5$

The oscillator's behavior is presented here for the value of T taken from the bifurcation diagram in the chaotic zone. This behavior is confirmed by a random evolution in the time response (figure 16). The phase portrait shows a multiplicity of periods (figure 17), confirmed by the appearance of several points on the Poincaré section.

b) Behavior at $T = 5$

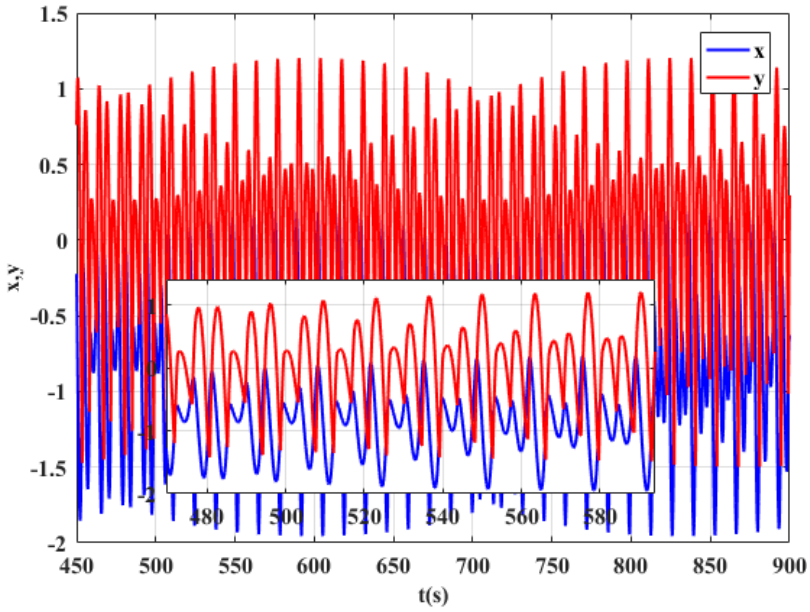

FIGURE 16 Temporal response at $T = 4.5$

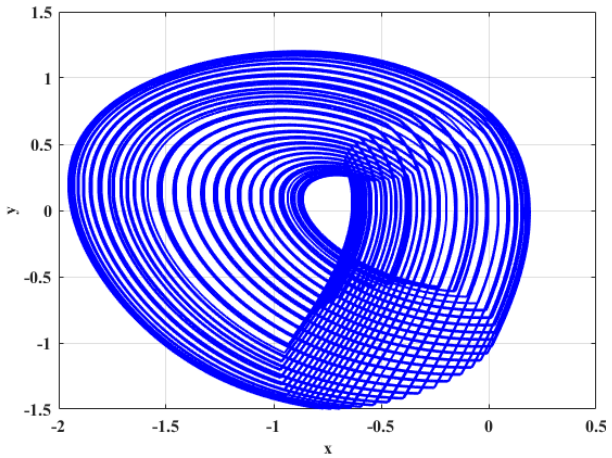

FIGURE 17 Phase portrait for $T = 4, 5$

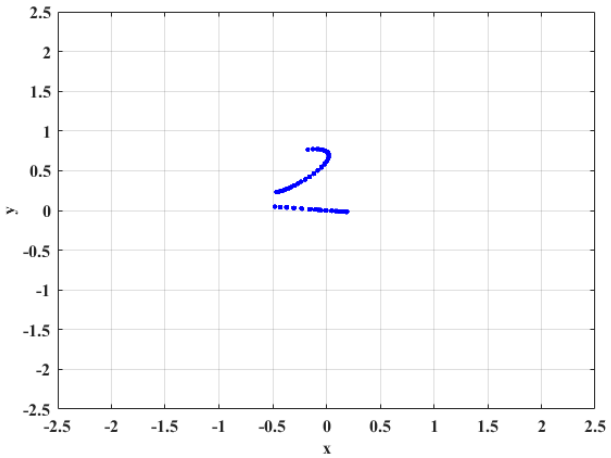

FIGURE 18 Poincaré section

The behavior presented here shows the dynamics of the oscillator at the value taken in the periodic zone, the time evolution shows a periodic regime. The phase portrait shows a limit cycle characteristic of fundamental periodic behavior (figure 17), which is confirmed by the presence of a single point on the Poincaré section (figure 18).

5.3 | Analysis of oscillator behavior under parameter variation B_1

5.3.1 | Bifurcation diagram

The bifurcation diagram presented here shows the evolution of state variables x under variation of the parameter B_1, which depends mainly on the circuit parameters (**DC voltage** E_1). simulations are performed over a range of B_1 values from 0 to 2.4 in steps of 2×10^{-3} . For each value of B_1 1700 periods of circuit operation were recorded with a resolution of 10000 points per period. In order to eliminate as many transient values as possible for each value of B_1, only the last 750 periods were retained for the diagram. For some values of B_1, we observe periodic behavior, from fundamental periodicity to chaos, passing through

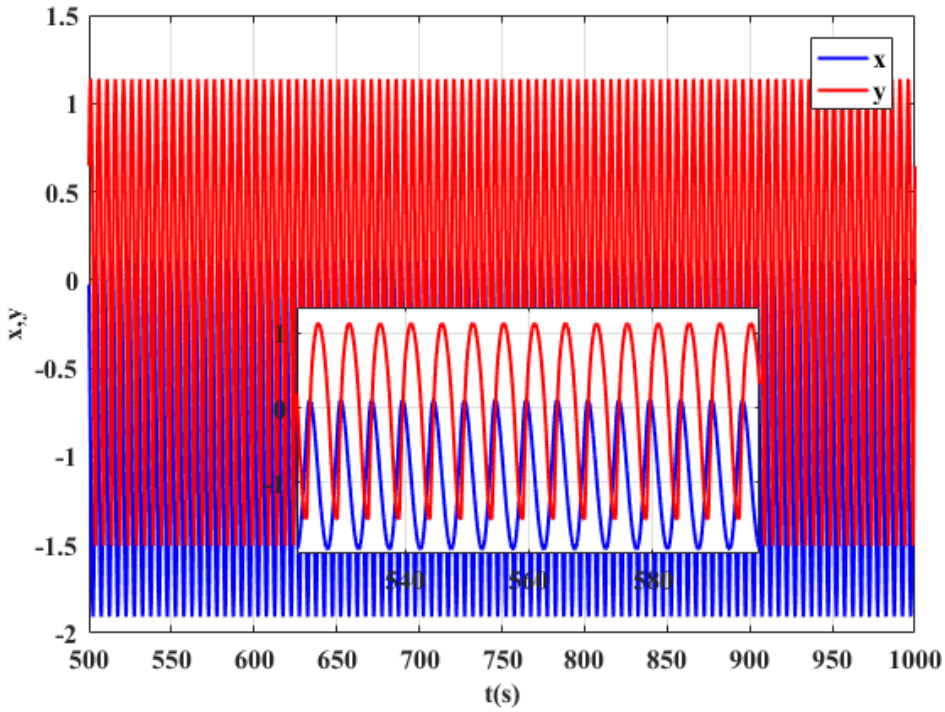

FIGURE 19 Time response at $T = 5$

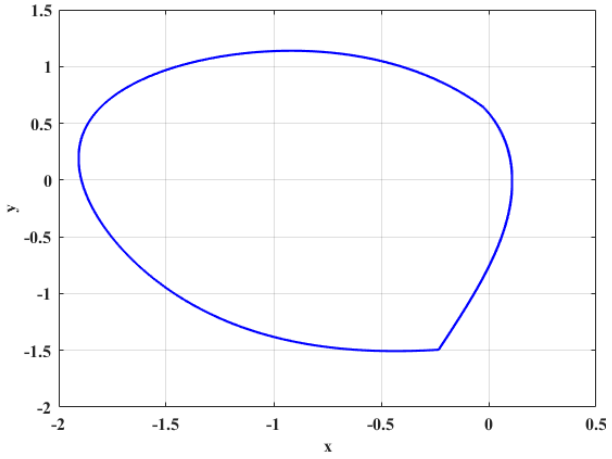

FIGURE 20 Phase portrait for $T = 5$

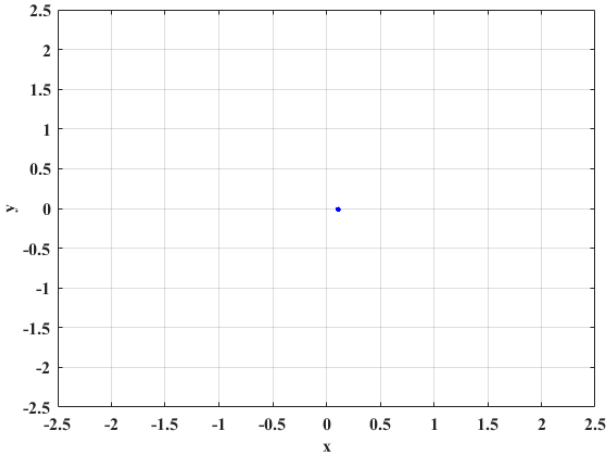

FIGURE 21 Poincaré section

windows of periodicity or subharmonic behavior of any rank. The behavior of the Alpazur oscillator is shown in figure 23 by the ME methods approach confirms when it's periodic for a value of zero ME and when it's chaotic for non-zero ME.

5.3.2 | Temporal responses

a) Behavior at $B_1 = 1.2$

The behavior at this value of B_1 taken from the bifurcation diagram in the periodic regime zone. The time trend shows a periodic evolution (figure 24). This behavior is confirmed by a limit cycle in the phase portrait (figure 25), which is characterized by the presence of a single point on the Poincaré section (figure 26).

b) Behavior at $B_1 = 2.01$

The behavior presented here is based on the value of B_1 taken from the bifurcation diagram in the chaotic regime zone. We observe a random regime marked by a multiplicity of periods given by the phase portrait (figure 28) and characterized by the appearance of several points on the Poincaré section (figure 29).

5.4 | Analysis of oscillator behavior under variation of parameter B_2

5.4.1 | Bifurcation diagram under variation of parameter B_2

The bifurcation diagram presented here shows the evolution of the state variable x under the variation of the parameter B_2 , this parameter depends mainly on the voltage E_2 of the circuit. Simulations are performed over a range of B_2 values from 0 to 5 in steps of 5×10^{-3} . For each value of B_2 1700 periods of circuit operation were recorded with a resolution of 10000 points per period. In order to eliminate as many transient values as possible for each value of B_2, only the last 750 periods were retained for the diagram. From this bifurcation diagram, we can see that for values of B_2 greater than 1.8, the Alpazur oscillator's circuit dynamics exhibit periodic behavior, which is justified by the value of ME being zero, while for a non-zero value of ME the behavior is chaotic (figure 31).

5.4.2 | Time responses

a) Behavior at $B_2 = 0.1$

The behavior is presented here at this value of B_2 taken in the periodic regime zone from the bifurcation diagram. We observe a sub-harmonic regime of rank 3 on the time evolution figure 32 . This behavior is confirmed by three cycles in the phase portrait (figure 33), characterized by the appearance of three points on the Poincaré section (figure 34).

b) Behavior at $B_2 = 0.06$

The behavior is presented here for the value of B_2 taken from the bifurcation diagram in the chaotic regime zone. We observe a random regime marked by a multiplicity of irregular cycles, presenting a strange attractor in the phase portrait (figure 36) characterized by the presence of several points on the Poincaré section (figure 37).

6 | CONCLUSION

In this paper we consider an Alpazur oscillator through investigation a multi-parametric way using chaos theory tools such as such as bifurcation diagram, Matching Energy technique, phase portrait, Poincaré section and temporal response. The results show that the Alpazur oscillator exhibits many behavior which can evolve from fundamental periodicity to chaos. This study therefore contributes to a deeper understanding of the various behaviors of this oscillator.

7 | BIBLIOGRAPHY

References

1. Edward N. L. Deterministic nonperiodic flow.. *Journal of atmospheric sciences* 1963; 20(2): 130–141.

2. Y. IN, Landa Polina S. Stochastic and chaotic oscillations. *Springer Science and Business Media* 1992; 77.

3. T. KM. Bifurcations and chaos in a model biochemical reaction pathway. *International Journal of Bifurcation and Chaos* 1998; 8(02): 381–394.

4. Yue M, H. K, Chi K. T. Bifurcation Analysis of Switched Dynamical Systems with Periodically Moving Borders. *IEEE trans. circuits and systems* june 2004; 51(6).

5. Yue M, H. K, Chi K. T, Takuji K. General Consideration For Modeling And Bifurcation Analysis of Switched dynamical systems. *IJBC* 2006; 16(3): 693–700.

6. Dong D, Chi K. T, Xikui M. Symbolic Analysis of Switching Systems: Application to Bifurcation Analysis of DC/DC Switching Converters. *IEEE trans. circuits and systems* August 2005; 52(8).

7. Chi K. T, al . Complex intermittency in switching converters. *International Journal of Bifurcation and Chaos* 2008; 18(1): 121–140.

8. Takuji K, Yutaka U, H. K. Bifurcation of nonlinear circuits with periodically operating switch. In: . 84. ; 2001.

9. Yutaka U, H. K. In: .

10. Kousaka T, all . Bifurcation analysis of a piecewise smooth system with non-linear characteristics. *International journal of circuit theory and applications* 2005; 33: 263–279.

11. T. K, all . Bifurcation analysis in hybrid nonlinear dynamical systems. *IEEE. 0-7803-6685* 2001; 9(1).

12. Takuji K, Tetsushi U, Yue M, H. K. Control of chaos in a piecewise smooth nonlinear system. *Chaos, Solutions and Fractals* 2006; 27: 1019–1025.

13. Kawakami H, René L. Structure and Bifurcations of Dynamical Systems. In: 1992.

14. Milne WE. Numerical solution of differential equations. *New York: Dover* 1970.

15. Butcher RC. A history of Runge-Kutta methods. *Applied numerical mathematics* 1996; 20(3): 247–260.

16. Julyan C, Piro O. The dynamics of Runge–Kutta methods. 1992.

17. Kousaka T, Ueta T, Ma Y, Kawakami H. Bifurcation analysis of a piecewise smooth system with non-linear characteristics. *International journal of circuit theory and applications* 2005; 33(4): 263–279.

How to cite this article: Williams K., B. Hoskins, R. Lee, G. Masato, and T. Woollings (2016), A regime analysis of Atlantic winter jet variability applied to evaluate HadGEM3-GC2, *Q.J.R. Meteorol. Soc.*, *2017;00:1–6*.

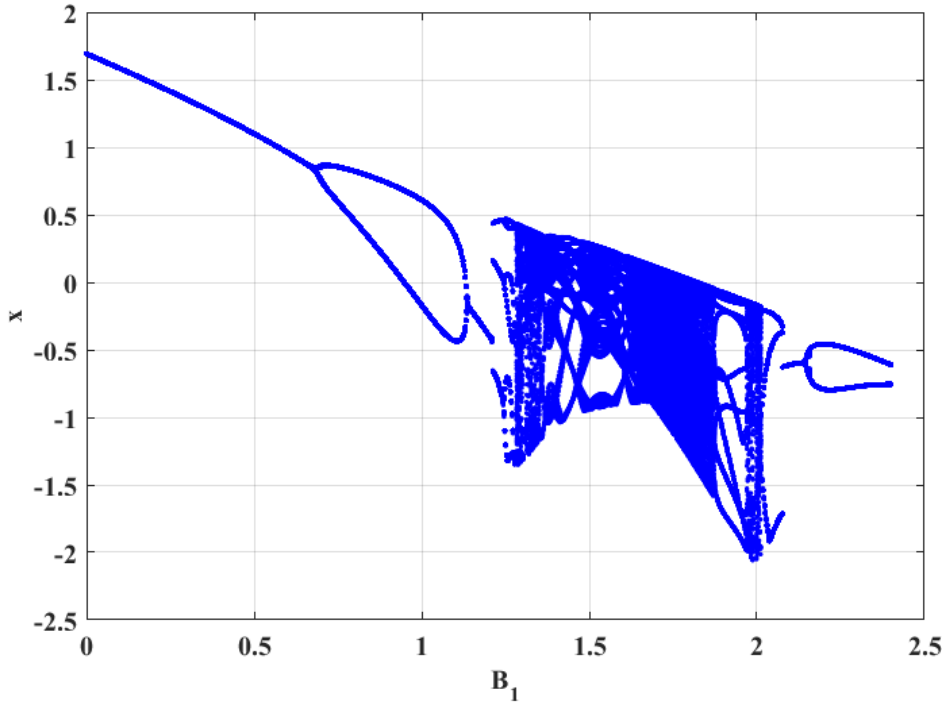

FIGURE 22 Bifurcation de x

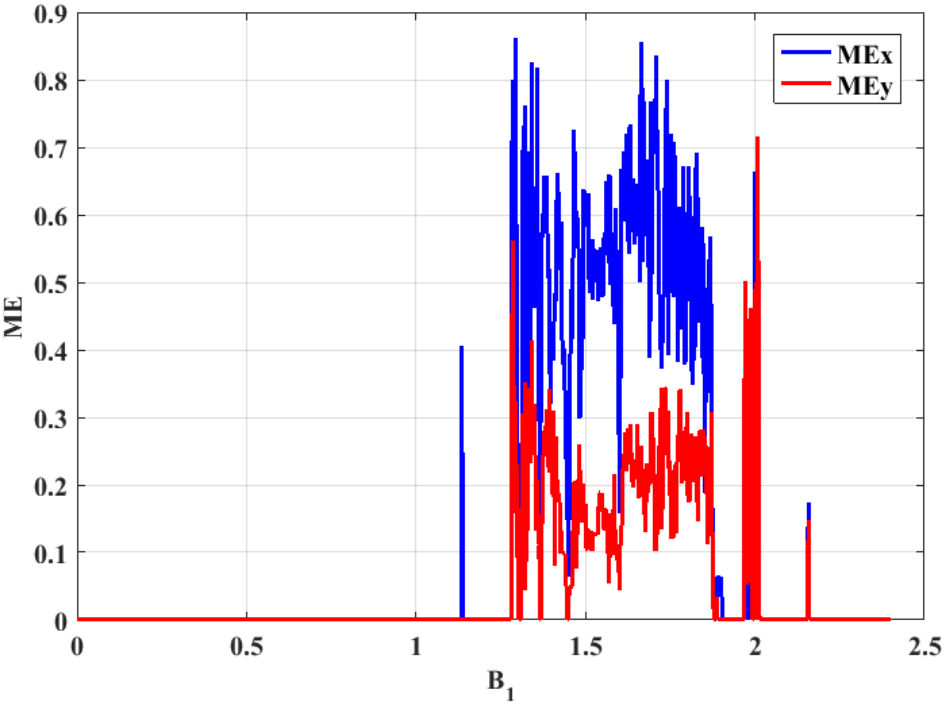

FIGURE 23 Matching Energy at θ

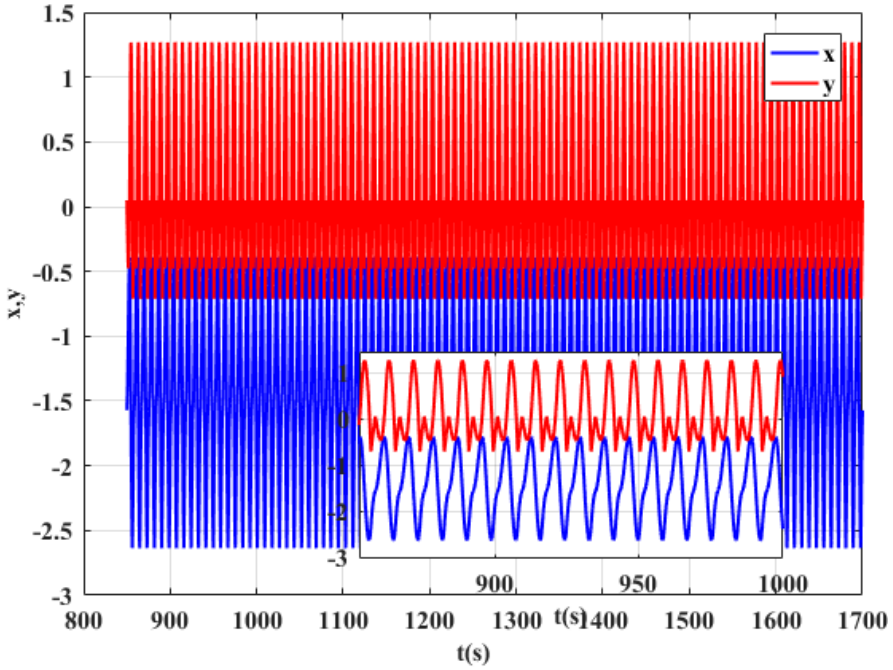

FIGURE 24 Temporal response for $B_1 = 1.2$

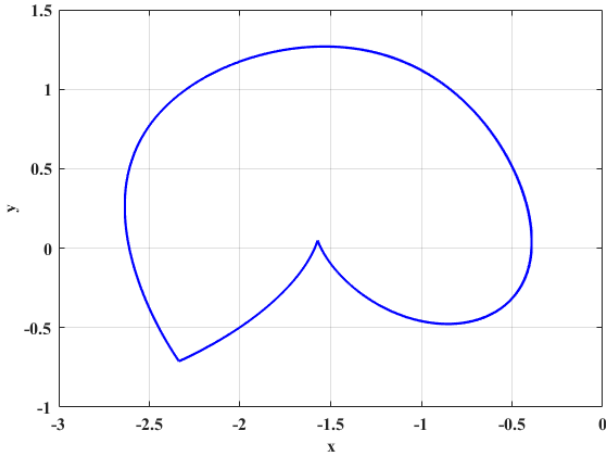

FIGURE 25 Phase portrait for $B_1 = 1, 2$

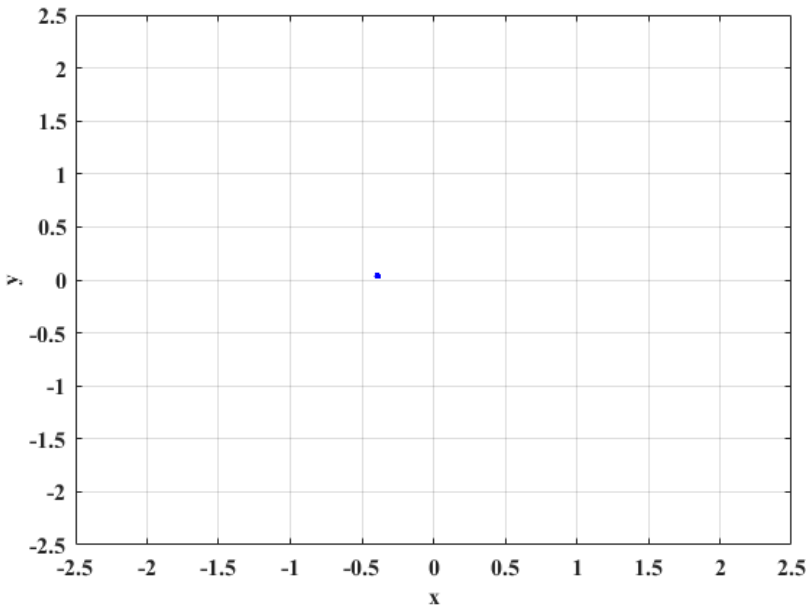

FIGURE 26 Poincaré section

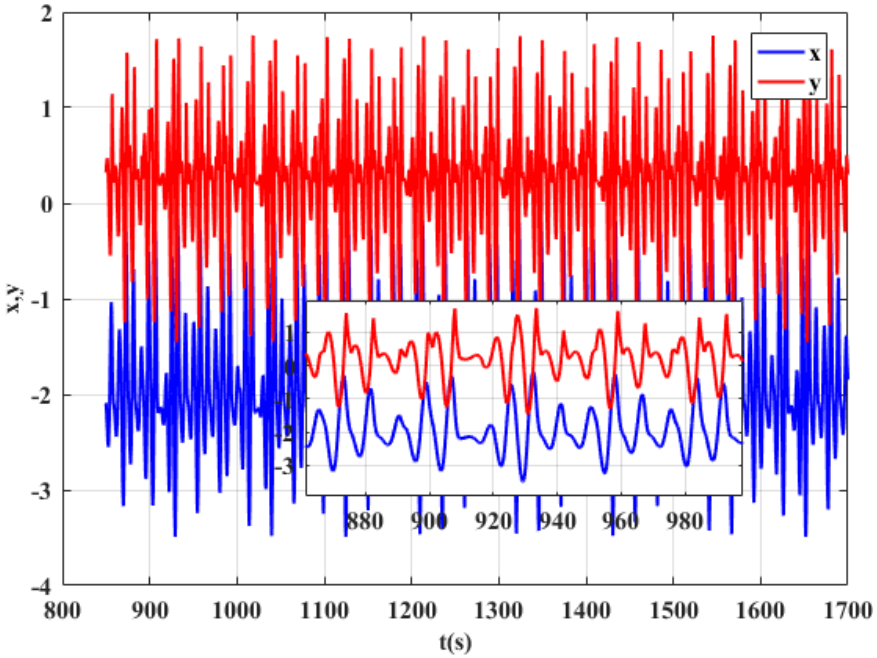

FIGURE 27 Temporal response for $B_1 = 2.01$

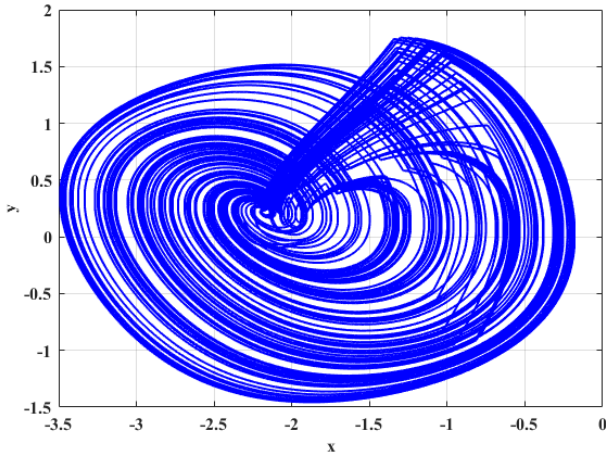

FIGURE 28 Phase portrait for $B_1 = 2.01$

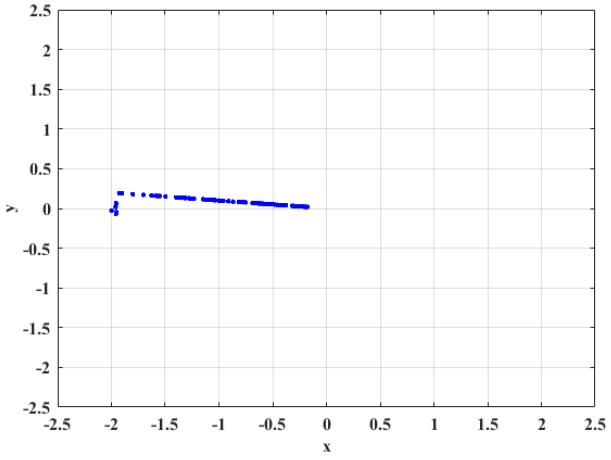

FIGURE 29 Poincaré section

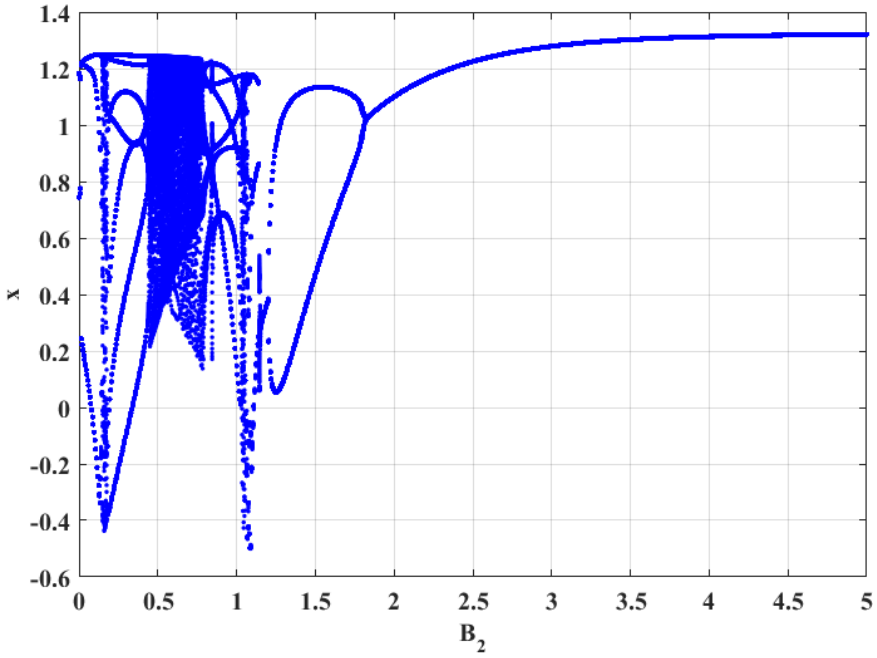

FIGURE 30 Bifurcation of x

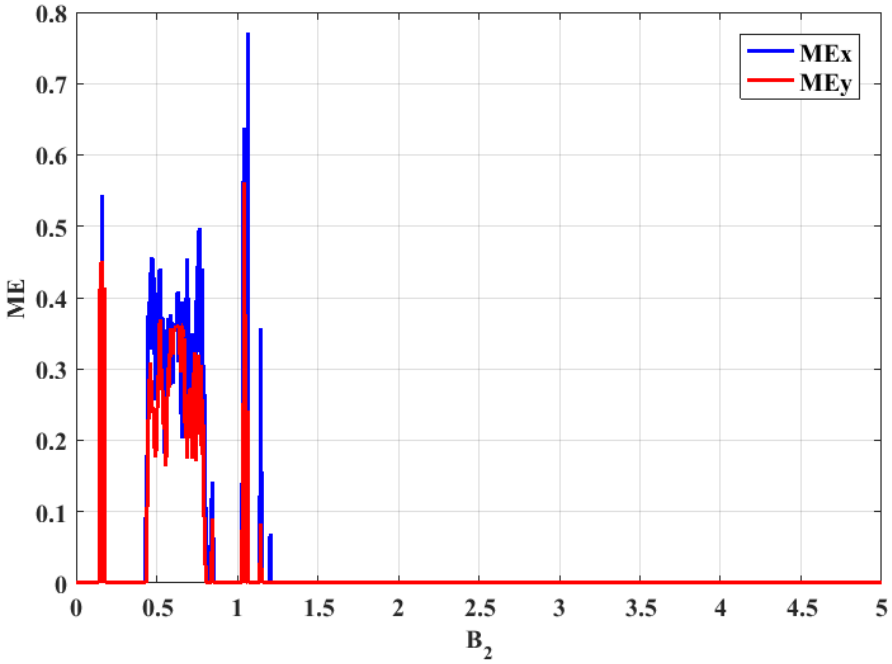

FIGURE 31 Matching energy sous θ

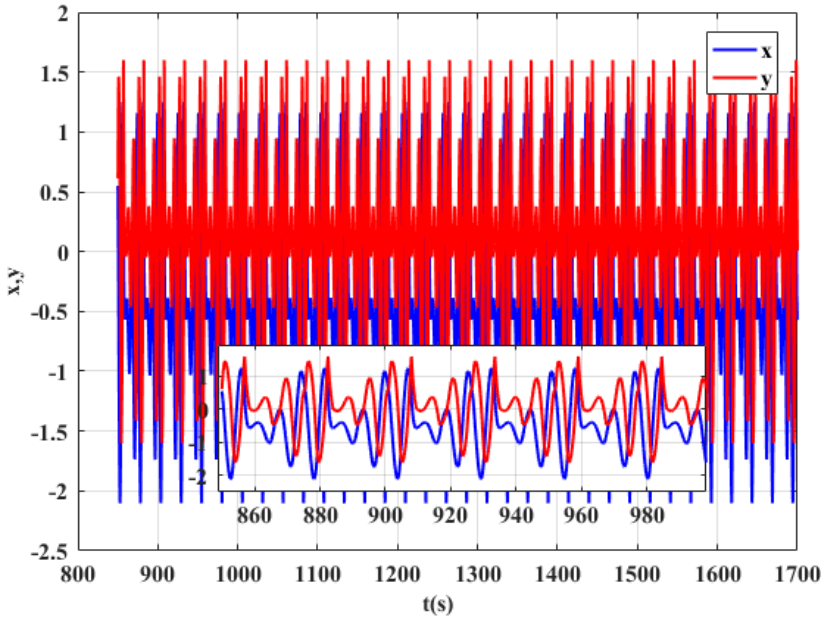

FIGURE 32 Temporal response for $B_2 = 0.1$

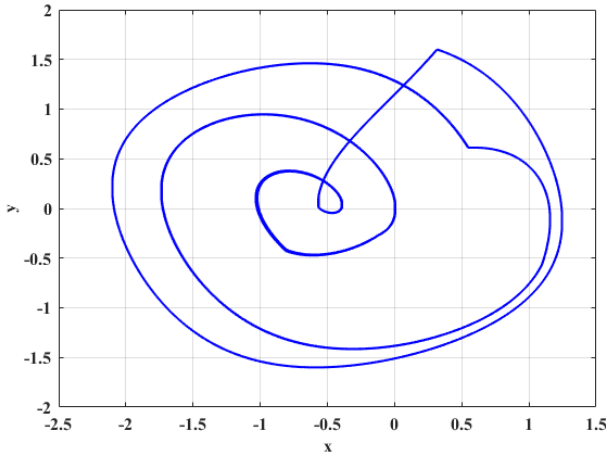

FIGURE 33 Phase portrait for $B_2 = 0.1$

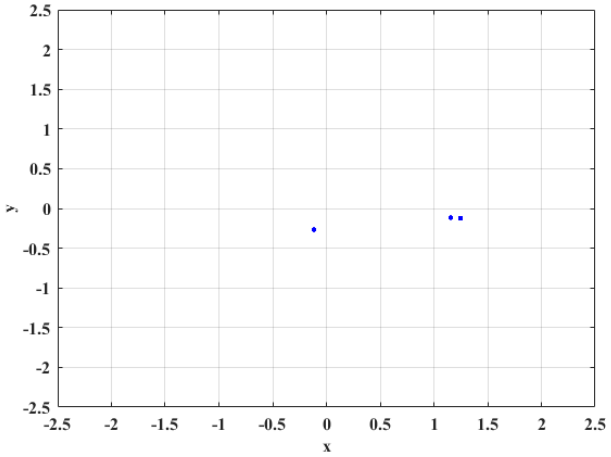

FIGURE 34 Poincaré section

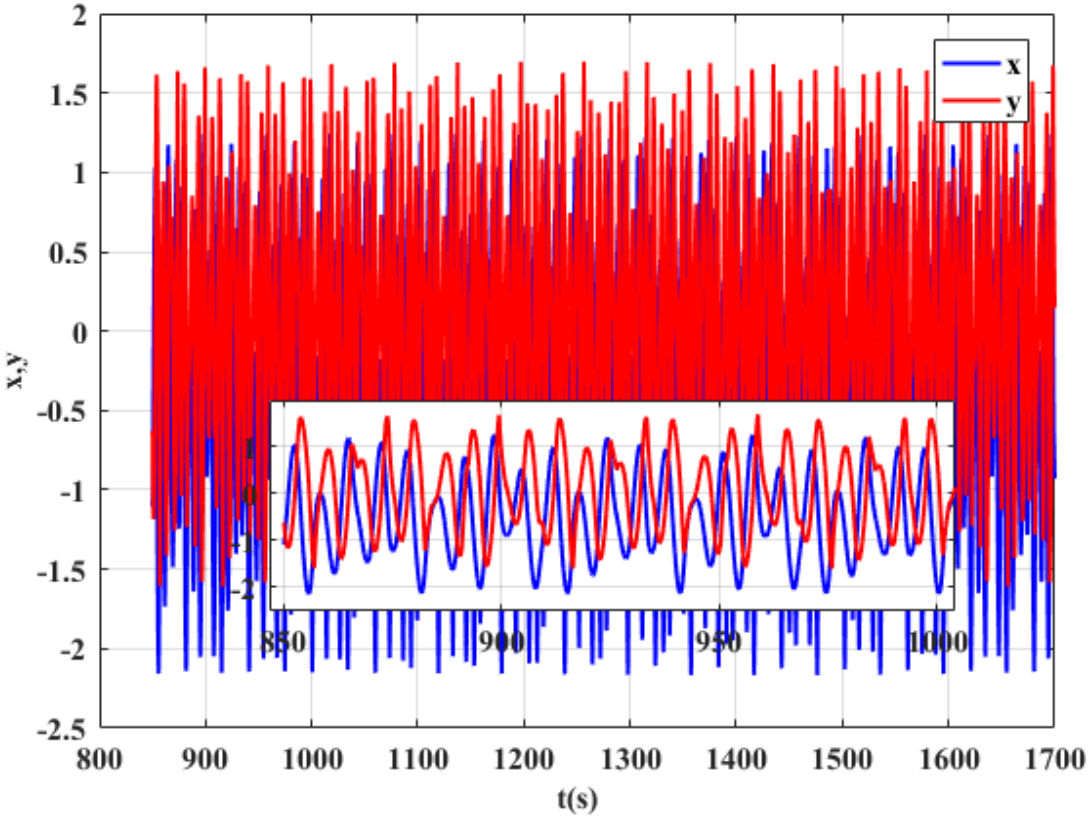

FIGURE 35 Temporal response for $B_2 = 0.6$

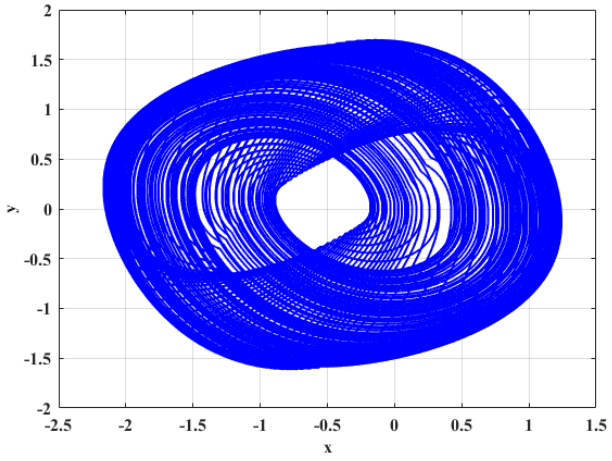

FIGURE 36 Phase portrait for $B_2 = 0.6$

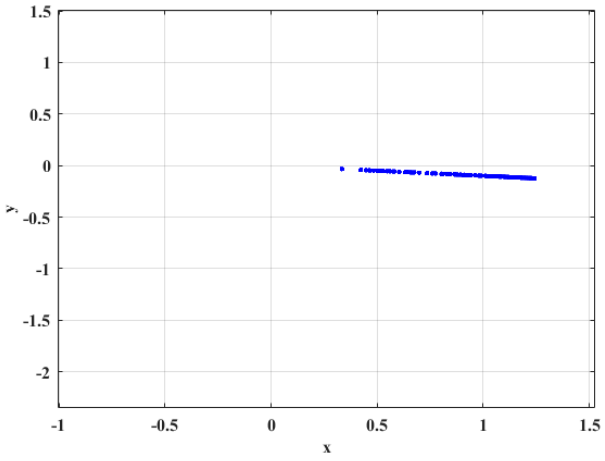

FIGURE 37 Poincaré section